Available online at www.sciencedirect.com
SCIENCE DIRECT
ELSEVIER
Earth-Science Reviews 75 (2006) 155–175
EARTH-SCIENCE REVIEWS
www.elsevier.com/locate/earscirev

Uranium-series dating applications in natural environmental science

Peter van Calsteren *, Louise Thomas

Department of Earth Sciences & OUUSF, The Open University, Walton Hall, Milton Keynes, MK7 6AA, USA

Received 2 March 2005; accepted 6 September 2005
Available online 19 December 2005

Abstract

Uranium-series (U-series) analyses are an essential component of many research projects in Earth and environmental science, oceanography, hydrology and science-based archaeology. Topics range from magma chamber evolution and volcanic hazard prediction, global climatic change through dating of authigenic carbonate deposits, human evolution through dating of bone, to the study of groundwater evolution. The U-series decay chains contain many elements that can be fractionated in environmental and geological processes. Half-lives of radioactive isotopes of such elements range from seconds to many millennia and application depends on the natural timeframe of the process or the elapsed time. This review will be limited to some aspects of the ^{238}U–^{234}U–^{230}Th–^{226}Ra system with half-lives of 245 kyr, 76 kyr and 1.6 kyr, respectively.

In environmental systems, fractionation of uranium and thorium is a very efficient process because thorium is extremely insoluble while hexavalent uranium in oxidising conditions is relatively soluble. Many authigenic precipitates of calcite contain virtually no thorium and inorganic precipitates have U/Ca ratios very similar to the ratio of dissolved uranium and calcium. Almost no radiogenic ^{230}Th in the precipitate means that the radiogenic clock starts effectively at zero. However, pure authigenic precipitates are rare and many contain some allogenic material, mostly silicate with ^{238}U in secular equilibrium with significant ^{230}Th. Some of the characteristics of different types of samples and various methods to accommodate or correct for 'inherited' ^{230}Th will be discussed.

Authigenic material should remain a 'closed system' with respect to the relevant isotopes but that requirement is sometimes difficult to maintain because radioactive decay results in damage to the crystal lattice of the host mineral. Consequences of this 'recoil effect' and correction schemes will be discussed. Dating archaeological bone based on the systematics of diffusion and adsorption to effectively model 'open system' behaviour is also included.

Keywords: uranium-series disequilibrium; dating; authigenic; allogenic; open-system; environment

1. Introduction

Uranium-series disequilibrium is a large and complex subject and this review cannot hope to be comprehensive, only a small selection of topics will be discussed, with emphasis on environmental applications. Some aspects of U-series are discussed in most isotope geochemistry textbooks and the most comprehensive treatment can be found in Ivanovich and Harmon (1982) and Bourdon et al. (2003).

There are two main reasons for dating environmental, geological and archaeological materials:

1. A precise age for a bone or a deposit underpins our understanding of its significance by establishing its archaeological or geological context.

* Corresponding author. Fax: +44 1908 655151.
E-mail addresses: p.v.calsteren@open.ac.uk (P. van Calsteren), e.thomas@open.ac.uk (L. Thomas).
URL: http://www2.open.ac.uk/ou-usf/ (P. van Calsteren).

0012-8252/$ - see front matter © 2005 Elsevier B.V. All rights reserved.
doi:10.1016/j.earscirev.2005.09.001

2. The time-span between two dates of samples that were deposited under different conditions makes it possible to calculate the rate of change and may indicate the process that caused the change.

Radiometric dating does not date an 'event' but can only give the time of an element fractionation process. The significance of the element fractionation process depends on the understanding of that process. A process that is fast relative to the time that has elapsed, may be an 'event' that can be 'dated'. U-series disequilibrium dating has many applications and any list will be incomplete but it maybe worthwhile considering U-series when deposits <350 kyr are studied.

^{238}U, ^{235}U and ^{232}Th decay to stable ^{206}Pb, ^{207}Pb and ^{208}Pb, with half-lives of 4.5 Gyr, 14 Gyr and 0.7 Gyr, respectively. The nuclear reactions to stable lead isotopes result from the expulsion of 8, 7 and 6 α-particles, respectively, and many intermediate β and γ reactions. Half-lives of intermediate reactions in these decay chains range from fractions of a second 245 kyr for ^{234}U. This review is somewhat arbitrarily limited to the decay systems of ^{234}U, ^{230}Th and ^{226}Ra with half-lives of 45 kyr, 76 kyr and 1.6 kyr, respectively.

The minor abundance uranium isotope ^{235}U decays to the protactinium isotope ^{231}Pa with a half-life of 32.8 kyr. Protactinium occurs in macroscopic quantities only in uranium ores and the geochemical characteristics of protactinium are difficult to determine but probably similar to those of thorium. An analytical method to purify protactinium from silicate rocks was published recently (Regelous et al., 2004), but applications are rare in recent years. ^{231}Pa is finding applications in coral dating (Mortlock et al., 2005; Edwards et al., 1997) and in oceanography (Moran et al., 2002, 2005).

Valid interpretations based on radiogenic isotope data require 'closed system' behaviour, where there is no exchange of any parent or daughter isotopes with the environment and the change in parent–daughter isotope ratio of the system is governed solely by the laws of radioactive decay. In that case, the age of the sample can be calculated with the decay equations. The time that can be calculated from the isotope ratio data is the time since the fractionation process that separated the parent from the daughter elements. If the fractionation process is efficient and fast relative to the half-life of the isotope in question, then it can be considered as an 'event' that can be dated. Potassium–argon dating of Mesozoic or older volcanic rocks is probably the simplest example. Argon degassing will have been efficient from hot lava and cooling through the argon retention temperature will have been quick, e.g. Yamamoto and Burnhard (2005).

To facilitate discussion, it will be helpful to adopt informal definitions of partition coefficient, and fractionation coefficient. The partition coefficient (PC) is here the ratio of the concentrations of an element, parent or daughter, before and after a fractionation process. In the example above, the potassium concentration does not change appreciably during the extrusion of the lava and the PC of potassium is close to unity. Argon loss during melting is also small but degassing of argon at atmospheric pressure after eruption of the lava is very efficient, resulting in much lower argon concentration in the lava than in the precursor and consequently, a large PC.

The fractionation coefficient (FC) is the ratio of the parent and daughter PCs. FC close to unity indicates little fractionation while an efficient fractionation process can be characterised by large or small FC. In this example, the K/Ar ratio in the precursor rock is much smaller than in the degassed lava. The resulting FC is not close to unity and degassing is an efficient K–Ar fractionation process.

1.1. Dating parent–daughter fractionation in silicate rocks

Many parent and daughter elements have similar geochemical characteristics, and similar PCs. For example, radioactive parent samarium and radiogenic daughter neodymium are both even-number Rare Earth Elements that rarely fractionate more than a few percent in any natural process. Similarly, total range of U/Pb ratios for almost all silicate rocks on Earth is only around 30% because FC is close to unity for partial melting and fractional crystallisation processes despite the fact that the PC for both uranium and lead can be quite small and concentrations vary by orders of magnitude between many common rock types. The PC for some minerals, such as zircon and monazite, is sufficient to fractionate U from Pb, but these minerals rarely occur in large enough quantity to affect the whole rock U/Pb ratio.

If FC is close to unity and the fractionation process is not very efficient, mathematical models and multiple samples can be used to calculate ages. The extent to which the data conform to the model gives confidence in the result. In some fractionation processes a mineral phase may emerge with an extreme PC, for example, high Rb/Sr in biotite and U/Pb in zircon and these minerals may well be exploited for specific dating purposes.

In silicate melt systems both uranium and thorium are quadrivalent and the FC for U/Th is very close to unity. Consequently, uranium and thorium fractionate appreciably only during small-fraction partial melting at high pressure in the mantle in the presence of garnet or clinopyroxene, two minerals with a somewhat larger PC for thorium than for uranium. The duration of such fractionation processes can be of the same order as the ^{230}Th half-life, and it can be very difficult to get meaningful ages on silicate melts or minerals. However, U-series data contain a wealth of information on the characteristics of the magma melting and transport processes (Spiegelman and Elliott, 1993).

The ^{230}Th daughter ^{226}Ra has a half-life of 1602 yrs and data for this sub-system provide useful information on crystal fractionation and magma chamber processes (e.g., Vigier et al., 1999; Blake and Rogers, 2005) for magma evolution studies and even hazard assessment.

2. Uranium-series in environmental systems

2.1. Parent–daughter fractionation in environmental samples

Both uranium and thorium are quadrivalent in the lithosphere but uranium becomes hexavalent under oxidising conditions. In environmental situations, hexavalent uranium is fairly soluble as $UO_2(CO_3)_3^-$ and similar ionic complexes whereas thorium remains quadrivalent and insoluble. The PC for thorium during weathering is large hence it remains in the mineral grains; however, PC for uranium is much smaller. Thus weathering of rocks and minerals results in efficient leaching of uranium into the water where it can be transported probably in the form of carbonic- or humic acid complexes. Thorium is highly particle-reactive and any small amount of dissolved thorium re-precipitates on particulate matter before it can be transported. Uranium is removed from water during the precipitation of carbonates and phosphates, but also when it returns to quadrivalent state under reducing conditions that occur with the accumulation of organic matter, including peat.

In environmental samples, U-series dating is mostly carried out in authigenic phases, i.e., minerals that were formed, or are precipitates in the system of interest. Uranium is incorporated in the mineral structure or simply co-precipitated. The main minerals are calcite and aragonite, both forms of $CaCO_3$. The mineral component of bone, hydroxyl-apatite, $Ca_5(PO_4)_3OH$ has a very strong affinity for uranium and this is also the case for environmental inorganic phosphates.

2.2. Sources and transport of uranium

Uranium concentrations in continental rocks range from 2 μg g^{-1} in sedimentary rocks to 4–10 μg g^{-1} in most granites, while the concentration in basaltic rocks such as ocean ridge basalts, is 2–3 orders of magnitude lower. The uranium concentration in soils is generally less than in the source rock, depending on soil type and maturity. Development of soil profiles is the most efficient process of rock break-down and vadose water with its relatively high P_{O_2} and P_{CO_2} is the main agent that accumulates and transports uranium as soluble $UO_2(CO_3)_3^-$ and similar ionic complexes. Vadose water contributes to phreatic water and depending on the P_{O_2} and P_{CO_2} in the aquifer, phreatic water may continue to leach uranium from the aquifer matrix, or uranium may precipitate where conditions become reducing. Phreatic water leaching can be a very efficient process and well-water can contain close to a μg g^{-1} uranium (e.g. Orloff et al., 2005). Vadose water also contributes to river water, but river-water usually contains <0.3 ng g^{-1} uranium, (Palmer and Edmond, 1993). Although there is potential for uranium to co-flocculate in estuaries, limited evidence indicates that uranium actually behaves conservatively, i.e., all the uranium that is dissolved in river water reaches the open sea and does not precipitate or flocculate during river–seawater mixing (Pogge von Strandmann et al., 2005). The uranium concentration in seawater is 3.3 ng g^{-1} in the open ocean (Chen et al., 1986).

2.3. Uranium–thorium fractionation

As discussed in Section 1.1, uranium and thorium fractionate very little in the silicate Earth. Th–U fractionation does take place in the hydrosphere because uranium is relatively soluble in water (see Section 2.1), but thorium is to all intents and purposes insoluble. The ^{232}Th concentration maybe up to 0.5×10^{-4} ng g^{-1} in seawater (Moran et al., 2002), five orders of magnitude lower than uranium. There is significant ^{230}Th, derived from ^{234}U decay in seawater, amounting to 0.7×10^{-8} ng g^{-1}. Thorium is highly 'particle reactive' but precipitation on particles appears to be an equilibrium process and 10–15% of ^{230}Th is actually in solution (Moran et al., 2002). A consequence of the particle-reactivity of thorium is that the total concentration of ^{230}Th increases with depth in the open ocean, while the uranium concentration remains fairly constant below the surface layer.

The effect of dissolved ^{230}Th on the age of authigenic carbonates is insignificant in shallow water where

it equates to a correction amounting to 1–2 yrs (Edwards et al., 1987). However, a correction is required for extremely slow-growing (mm/Myr) manganese nodules in deep oceans (Henderson and Burton, 1999).

^{232}Th concentration in fresh water is so low that it is difficult to measure but probably also five orders of magnitude less than uranium (Reynolds et al., 2003) if the river does not drain a hydrothermal area. Groundwater may contain 10 times more thorium than riverwater.

The Th/U ratio in pure hydrothermal calcite can be close to unity (Grimes et al., 1998) and this has been interpreted to indicate that, in hot hydrothermal water, the solubility of thorium is much higher than at ambient temperature and may approach uranium solubility.

3. U-series dating

3.1. U-series systematics, introduction

U-series nuclide relations are best illustrated on a simplified Nuclide Chart (Fig. 1) which indicates the atomic or proton number N of the elements that determines the chemical properties, and the isotopic number Z that is approximately the same as the mass number of an isotope (given as a superscript to the left of an element symbol) and determines the physical properties. Decay reactions are indicated by arrows.

The law of radioactivity states that the number of atoms disintegrating per unit time is proportional to the number of radioactive atoms N.

Thus:

$$-\mathrm{d}N/\mathrm{d}t = \lambda N \tag{1}$$

where λ is the proportionality or decay constant and N is the number of radioactive nuclei.

On integration this becomes:

$$N = Pe^{-t\lambda} \tag{2}$$

where P is the number of radioactive parent isotopes at the time of the formation of the sample, N is the number present today and e is the base of the natural logarithm.

The number of radiogenic daughter isotopes, D, plus the number of radioactive parent isotopes P is equal to N and Eq. (2) may be rewritten as:

$$D = P\left(1 - e^{-t\lambda}\right) \tag{3}$$

In many cases, there is an initial abundance of daughter isotopes (D_i) already in the system. For convenience, all factors are divided by the abundance of a stable isotope (S). The equation then becomes:

$$\frac{D}{S} = \frac{D_\mathrm{i}}{S} + \frac{P}{S} \times \left(1 - e^{-t\lambda}\right) \tag{4}$$

In a decay-chain the radiogenic daughter decays further and a term of similar form to Eq. (2), with appropriate P, D and S isotopes, is introduced. Neither ^{232}Th, nor ^{238}U in other equations, are stable in a strict

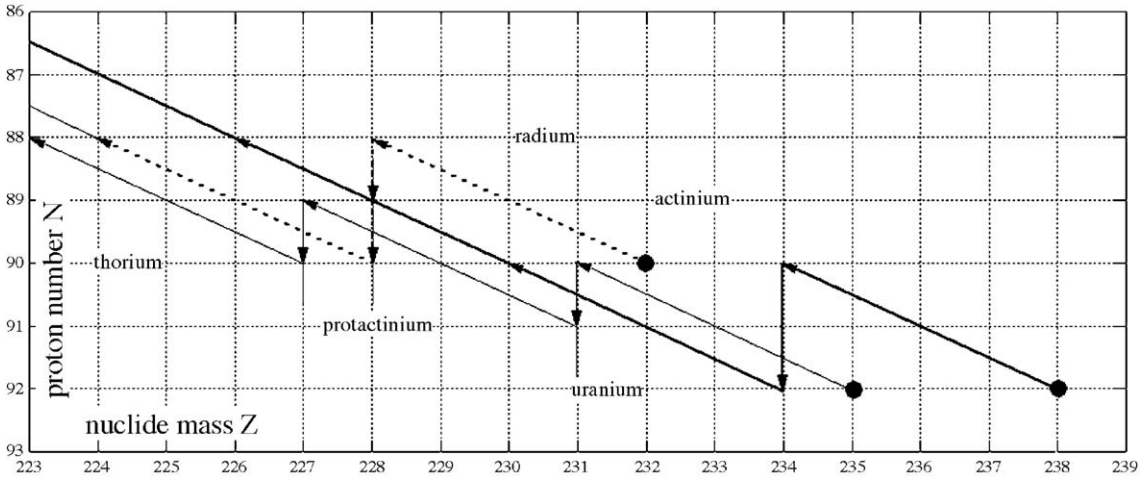

Fig. 1. Simplified chart of the nuclides for the U-series decay chains: ^{238}U-chain = heavy lines; ^{235}U-chain = thin lines; ^{232}Th-chain = dashed lines. Only nuclides with a half-life relevant to this review are included. Nuclide mass 'Z', also known as the 'isotopic weight' is plotted horizontally and proton number 'N' which determines the chemical element, is plotted vertically. α decay means a mass loss of an α particle of mass 4 and shift to lower Z, i.e., ^{238}U to ^{234}Th, as well as lower N, i.e., ^{92}U to ^{90}Th. β decay where a neutron of mass 1 transforms into a proton of mass 1 with the loss of an electron, mass 0, results in the increase of the proton number. An example of two β decays is the transformation of ^{234}Th to ^{234}U. ^{238}U, ^{235}U and ^{232}Th decay ultimately to stable isotopes of lead, ^{206}Pb, ^{207}Pb and ^{208}Pb, respectively.

sense but their half-lives are many orders of magnitude longer then the time-scales of U-series disequilibrium and both ^{232}Th and ^{238}U can be considered stable for practical purposes.

Written out for ^{230}Th, assuming the initial ^{230}Th/^{232}Th=0, the equation is:

$$\left(\frac{^{230}\mathrm{Th}}{^{232}\mathrm{Th}}\right)_t = \left(\frac{^{230}\mathrm{Th}}{^{232}\mathrm{Th}}\right)_i \times \left(e^{-t\lambda}230\right) + \left(\frac{^{234}\mathrm{U}}{^{232}\mathrm{Th}}\right)_i \times \left(1 - e^{-t\lambda}230\right) \quad (5)$$

which is known as the isochron equation.

A characteristic of the U-series methods is that after about 5 half-lives of ^{234}U, the nuclide with the longest half-life, the system is in 'secular equilibrium'. This means that all nuclides in a chain decay at the same rate and their isotope ratios are the same as the ratios of their decay constants. Consequently, initial ratios are known at the time of the element fractionation process. For convenience the isotope abundances can be expressed in terms of 'activity', A, the product of the abundance, C, and the decay constants of the nuclides, for example:

$$A^{230}\mathrm{Th} = \lambda^{230}\mathrm{Th} \times C^{230}\mathrm{Th} \quad (6)$$

In secular equilibrium all activities are equal to 1. Activity ratios are contained in brackets to distinguish these from isotope abundance ratios. U-series data can be displayed on an 'activity diagram', for instance (^{230}Th/^{232}Th) vs. (^{238}U/^{232}Th), Fig. 2, and there is no difference in principle, only in scaling with conventional radiogenic isotope diagrams. In secular equilibrium, a system may have (^{230}Th/^{232}Th) and (^{238}U/^{232}Th) as indicated by WR. A fractionation process such as the fast crystallisation of minerals in an extruding lava, could results in three mineral phases, A, B and C with different (^{238}U/^{232}Th) but the same (^{230}Th/^{232}Th) because heavy isotopes of the same element are not significantly fractionated at high temperatures. With time, ^{230}Th changes by radioactive decay. For mineral A there is excess ^{230}Th relative to its parent isotope and more will decay than is generated, while minerals B and C have a deficit and the opposite is the case. The (^{230}Th/^{232}Th) of the three phases evolves in the direction of the arrows until secular equilibrium is achieved again and all three phases plot on the equiline. This diagram is similar to an isochron diagram where the slope of a straight line may have age significance. The line with a slope of unity where the rate of radioactive production of an isotope is equal to its rate of decay is known as the 'equiline' and indicates systems in secular equilibrium or 'infinite' U-series age. ^{234}U–^{230}Th dating is limited to ~350 kyr, five half-lives of ^{230}Th and ^{230}Th–^{226}Ra dating is limited to 5 half-lives of ^{226}Ra or ~8000 yrs. Lower limits depend on daughter isotope ingrowth to a measurable quantity which requires about a century for ^{230}Th and a decade for ^{226}Ra.

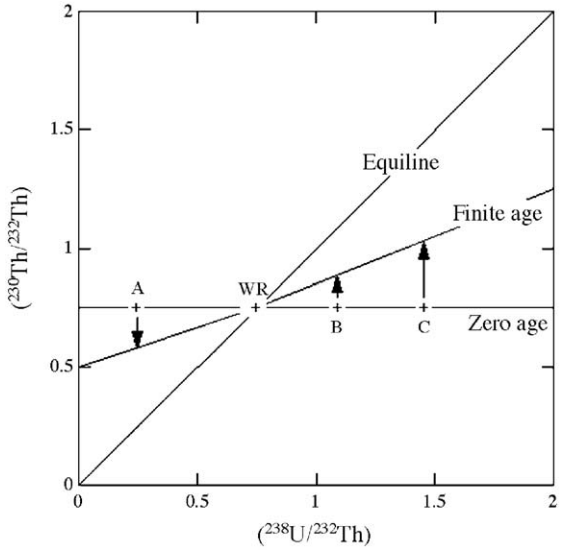

Fig. 2. Activity diagram, also known as an equiline diagram, illustrating U-series evolution. In secular equilibrium, a system may have (^{230}Th/^{232}Th) and (^{238}U/^{232}Th) as indicated by WR. A fractionation process results in three phases, A, B and C with different (^{238}U/^{232}Th) but the same (^{230}Th/^{232}Th). With time, the (^{230}Th/^{232}Th) of the three phases evolves in the direction of the arrows until secular equilibrium is achieved again and all three phases plot on the equiline.

Ages for authigenic minerals can be calculated for single samples on the assumption that all ^{230}Th has been produced by in situ decay of ^{234}U and there is no allogenic or initial ^{230}Th and no isotope redistribution within the system or exchange with the environment. Eq. (7) was derived by Kaufman and Broecker (1965).

$$\left(\frac{^{230}\mathrm{Th}}{^{234}\mathrm{U}}\right) = \left(\frac{^{238}\mathrm{U}}{^{234}\mathrm{U}}\right) \times \left(1 - e^{-T\lambda_{230}}\right) + \left\{\lambda_{230}/(\lambda_{230}-\lambda_{234})\right\} \times \left\{1 - \left(\frac{^{238}\mathrm{U}}{^{234}\mathrm{U}}\right)\right\} \times \left\{1 - e^{-T(\lambda_{230}-\lambda_{234})}\right\} \quad (7)$$

This equation is solved iteratively for T and equality can be approached to any required degree of accuracy. For T=0, (^{230}Th/^{234}U)=0 and after five half-lives of ^{230}Th, (^{230}Th/^{234}U) is 0.2% from equilibrium. The evolution of (^{230}Th/^{234}U) with time is plotted in Fig. 3a.

Total uncertainty in a calculated age is calculated by taking the square root of the sum of the squares of the analytical uncertainties in isotope abundance and isotope

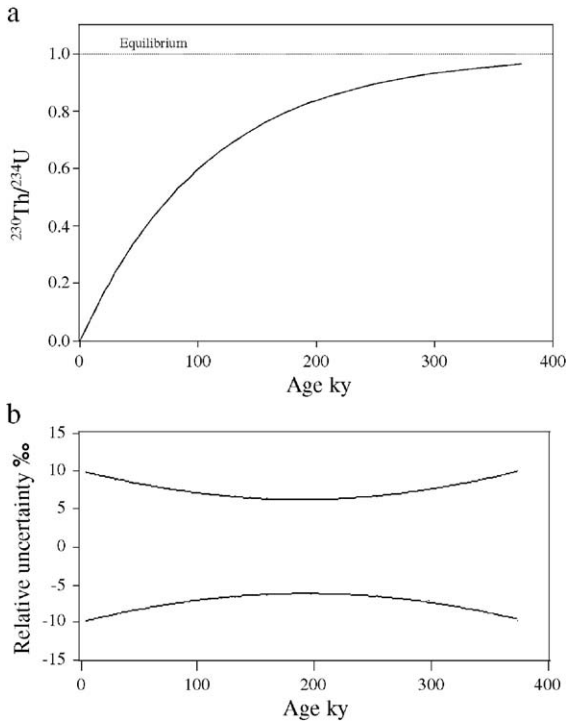

Fig. 3. (a) Evolution of (^{230}Th/^{234}U) with time, approaching equilibrium to approximately 0.2% after 5 half-lives of ^{230}Th, or 380 ky. (b) An illustration that uncertainty in (^{234}U/^{238}U)–(^{230}Th/^{234}U) ages increases at both extremes of the range. Example calculations are based of simulated values for (^{234}U/^{238}U) and (^{230}Th/^{234}U) and a constant analytical uncertainty of 0.2% for (^{234}U/^{238}U) and varying from 1% to 0.04% for (^{230}Th/^{234}U) from low to high ages, respectively.

ratio determinations, however, the form of Eq. (7) makes it difficult to use this method. Uncertainty in calculated ages can be illustrated by using assumed (^{230}Th/^{234}U) and (^{234}U/^{238}U) values for a range of ages from near zero to 400 kyr and adding or subtracting typical analytical uncertainties from these values. The (^{234}U/^{238}U) value is always fairly close to unity and a constant uncertainty of 0.2% is used. The ^{230}Th value in (^{230}Th/^{234}U) is zero at zero age and because a large part of the uncertainty is determined by counting statistics on the ^{230}Th intensity, in this illustration the assumed analytical uncertainty varies from 1% at 100 yrs to 0.04% at 380 kyr. Calculated uncertainty increases again when the calculated age approached five half-lives of ^{230}Th because a small variation in (^{230}Th/^{234}U) is equivalent to a large variation in age, as can be deduced from Fig. 3a. Results of uncertainty calculations are illustrated in Fig. 3b for the variables above.

3.2. Analytical techniques

There are two principal methods to quantify uranium, thorium and radium concentrations and isotope ratios. Alpha spectrometry is based on the intrinsic radioactivity of these nuclides and uses charged particle detectors that give information on the detected energy which identifies the nuclear disintegration reaction, and the intensity which can be used for quantification. Nuclides with short α half-lives and, therefore, many nuclear disintegrations per unit time, are best suited to alpha spectrometry. Equally, nuclides with short α half-lives have low abundances at any one time and are not suitable for mass spectrometry where nuclear abundance ratios are measured. Both techniques require at least some form of purification and pre-concentration and a number of chemical techniques are used.

3.2.1. Alpha spectrometry

Alpha spectrometry use either solid-state doped-silicon detectors or liquid scintillation detection with immiscible organic reagents for element-specific extraction and scintillation. Both methods are commonly used in environmental pollution applications where anthropogenic nuclides (plutonium, americium, neptunium, curium) with relatively short half-lives, are the main focus. Alpha spectrometry is also used for the quantification of ^{210}Po with applications, among others, in volcano degassing studies (Le Cloarec et al., 1992).

Alpha spectrometry equipment consists of a counting chamber that is evacuated to a level that minimises α-particle adsorption in air while also minimising implantation in the detector. The detector is usually a silicon diode with a near-surface (50 nm) layer implanted with Boron. Because α-particles are easily stopped by collision with matter, the window that protects the detector is extremely thin and samples are presented to the detector in a mono-molecular layer on a planchet. Output from the detector is analysed in a multi-channel analyser and evaluated by dedicated software for nuclide and intensity, as well as decay, interference, bias etc. The sensitivity range of alpha spectrometry is such that environmental ^{226}Ra with a half-life of 1602 yrs and nuclides with shorter half-lives, can be confidently quantified. The sensitivity of radium in TIMS and the much longer half-lives for naturally occurring ^{234}U, ^{230}Th and ^{231}Pa mean that mass spectrometry is usually preferred for these isotopes. Alpha spectrometry equipment is considerably cheaper than mass spectrometers and relatively simple to set-up and operate.

3.2.2. Mass spectrometry

Four different mass spectrometry techniques are in common use: thermal ionisation (TIMS), plasma ionisation using a quadruple mass filter (ICP–QMS) and plasma ionisation using a sector magnet with a single

detector system (SD–ICP–MS) or a multi-collector system (MC–ICP–MS). In all instruments, the nuclides of interest are ionised, separated according to mass and detected using either Faraday collectors of Ion Multipliers in analogue or ion-counting mode. A thorough discussion of the merits of these systems can be found in Platzner et al. (1997) but a few salient points are below.

ICP-based systems have orders of magnitude better sensitivity than TIMS systems for uranium and thorium which both have high ionisation potential, radium however, has a low ionisation potential and very much better sensitivity on TIMS.

The $^{234}U/^{238}U$ and $^{230}Th/^{232}Th$ ratios in silicate-derived samples are extreme, of the order of 5×10^{-5} and 5×10^{-6}, respectively. Abundance sensitivity, the 'tail' of a high abundance isotope on its neighbouring masses, is sufficiently high that a filter is required to significantly reduce the tail. Practical devices all reject ions with deviant properties using ion beam deceleration (Calsteren and van Schwieters, 1995). ICP–QMS is not suitable for this technique.

Instrumental mass-dependant isotope fractionation affects ICP-based systems an order of magnitude more strongly than TIMS. Correction using internal known ratios is impossible for thorium and radium and impractical for uranium because the invariant $^{238}U/^{235}U$ ratio of 137.88 is rather larger than optimal. Addition of a spike with known isotope ratio is possible for uranium and thorium but the amount of radioactive material that has to be added to make a statistically significant improvement in the data quality is large enough to be impractical on radiation safety grounds, in most laboratories. A fractionation correction is usually carried out based on the results of known standards that are analysed with the same protocol at frequent intervals between samples. Higher sensitivity of MC–ICP–MS relative to TIMS for most applications is an advantage; however, the much smaller fractionation correction in TIMS is an advantage if sample size, and therefore beam intensity, is not a limiting factor.

3.3. Chemical methods

Environmental samples rarely contain uranium, thorium or radium levels above $\mu g\ g^{-1}$ level and chemical methods are required to purify and concentrate sufficient quantities for U-series analysis. ICP–QMS methods are sensitive enough to detect and quantify ^{238}U or ^{232}Th, but not the low abundance isotopes. Sampling procedures have to be appropriate for the purpose and designed to minimise contamination. Sampling protocols can be summarised through two very simple examples of sampling of solids or water. A quantity sufficient to be representative of solid material is ground to a fine powder and dissolved in mineral acids. Uranium and thorium can be pre-concentrated from water samples using co-precipitation and the solids can be separated using centrifugation or filtration and dissolved in mineral acid. The elements of interest are separated from the mineral–acid solution using simple ion exchange chromatography or extraction techniques. Individual element samples are loaded on filaments for TIMS, taken up in weak acid solution for ICP and electro-plated or precipitated on a planchet for alpha spectrometry. Chemical procedures have to be carried out in dedicated laboratories designed to minimise contamination and to comply with Health and Safety and Radiation Safety requirements.

3.3.1. Laser ablation

Sensitivity of MC–ICP–MS is such that meaningful isotope ratios can be obtained from some environmental solid material using laser ablation, with minimal sample pre-treatment. The inherent small sample size means that uncertainty is higher then can be achieved with larger sample sizes using chemical separation methods, but information can be related directly to a micrometer-sized area of the sample. The technique has been successfully applied to a series of corals over the full U-series age range with examples of ages of 3 ± 1 ka and 125 ± 7 ka (Potter et al., 2005).

3.4. Quality control

All these analytical methods are to some extent relative and the analysis with the same protocols of suitable laboratory standards to assess reproducibility and of Certified International Reference Materials or their traceable derivatives, to assess accuracy is essential. The extremely high sensitivity of modern analytical equipment means that reagent and method blanks must be rigorously monitored and controlled. Regulatory requirements for the use of radioactive materials demand total sample containment and thorough accounting procedures.

U-series has a 'built-in' quality control check because samples that have remained closed-systems and are more than a million years old are in secular radioactive equilibrium, and must plot, within analytical uncertainty, on the equiline. To achieve this confirms that isotope ratio measurements as well as the spikes and standards that are used for quantification, are correctly calibrated.

4. U-series dating in environmental science applications

There are many approaches to dating environmental processes beyond the reach of historical records, all with specific applications and disadvantages. Two methods are based on the physical process of radioactive decay and are independent of correlations with other records; they are sometimes referred to as 'absolute' where other methods are 'relative'. Dating using ^{14}C depends on the availability of organic carbon, usually in the form of reduced carbon. Uranium-series disequilibrium dating depends mainly on the co-precipitation of uranium with authigenic minerals.

There are a number of assumptions specific to U-series dating:

(1) It is usually assumed that precipitation of the authigenic phase is a fast process, relative to the time that has elapsed since. This assumption is scale dependant in deposits that grow over time, where growth is more or less obvious from the presence of laminations. The fast-precipitation assumption holds easily where a lamina is the result of precipitation during one season, but care must be taken if the sampling is extended over a number of laminae. The calculated age will always be an average but the time gap between laminae must be evaluated.

(2) An authigenic phase that is dated does not contain any allogenic ^{230}Th, or this initial inherited ^{230}Th in the sample can be corrected. There are a number of ways of correcting for the allogenic contribution, some of which are discussed in Section 4.1, taking lake sediments as an example of methods that are applicable for many other types of samples. Correcting for allogenic ^{230}Th inevitably increases the overall uncertainty and a large correction on young samples can render an age meaningless.

(3) Daughter isotope loss from authigenic phases is evident because ($^{234}U/^{238}U$) is disturbed. It is usually assumed that initial ($^{234}U/^{238}U$) for seawater precipitates is in equilibrium with the seawater value of 1.145. This is a fair assumption for seawater where ($^{234}U/^{238}U$) = 1.145 has remained constant over the lifetime of ^{230}Th, (Henderson, 2002). However, in groundwater precipitates, ($^{234}U/^{238}U$) can vary over a wide range (Reynolds et al., 2003). This is discussed in more detail in Section 5 with methods for evaluating and correcting limited uranium loss.

(4) Gradual uranium uptake in archaeological bone is a reproducible process and can be modelled in terms of diffusion of uranium-ions into the bone structure and adsorption of uranium and its daughter nuclides by the fine-grained bone material.

Given the limitations of this review, it is probably effective to discuss various aspects of U-series disequilibrium dating in the context of appropriate examples such as fresh-water lake precipitates, speleothems, 'organic' carbonate and bone. There are many more types of materials that are amenable to U-series disequilibrium dating and many are discussed in Ivanovich and Harmon (1982) and Bourdon et al. (2003).

4.1. Marl

Shallow fresh-water lakes in limestone areas usually have bottom sediments often referred to as marls that consist of fine-grained limestone detritus and authigenic carbonate precipitate. Fresh-water precipitates contain uranium from the riverine input and tend to be relatively low in uranium, unless the rivers also drain a high uranium basement geology such as black shale (Israelson et al., 1998) or granite. Pore-water in marls becomes reducing from the decay of organic matter usually close to the water–sediment interface and this stabilises the uranium, (Cochran et al., 1986; Thomson et al., 2001). Marls can be a very useful environment archive (fossils, pollen, $\delta^{18}O$ and $\delta^{13}C$) because bioturbation tends to be limited in the reducing environment below the water–sediment interface.

Results from lacustrine sediments from Hawes Water (NW Lancashire, UK), Fig. 4, show a correlation of U-series ages with significant pollen horizons as environmental indicators. Hawes Water is a small shallow lake, where variations in climate and hydrological conditions are quickly reflected in the sediments. U-series ages match with a proxy chronology based on the pollen horizons and stable isotopic data. Trace element and stable isotope data for the Holocene sequence at Hawes Water indicate considerable climatic change during the last 10 kyr contrary to popular belief that the Holocene in NW Europe since the Younger Dryas as been a climatologically quiet period (Marshall et al., 2002).

It appears mainly from unpublished data that emergence and drying of marls results in oxidation of uranium which can then be washed out by meteoric and vadose water percolation. The best material is obtained by taking cores in actual lake sediments rather than sampling emerged deposits.

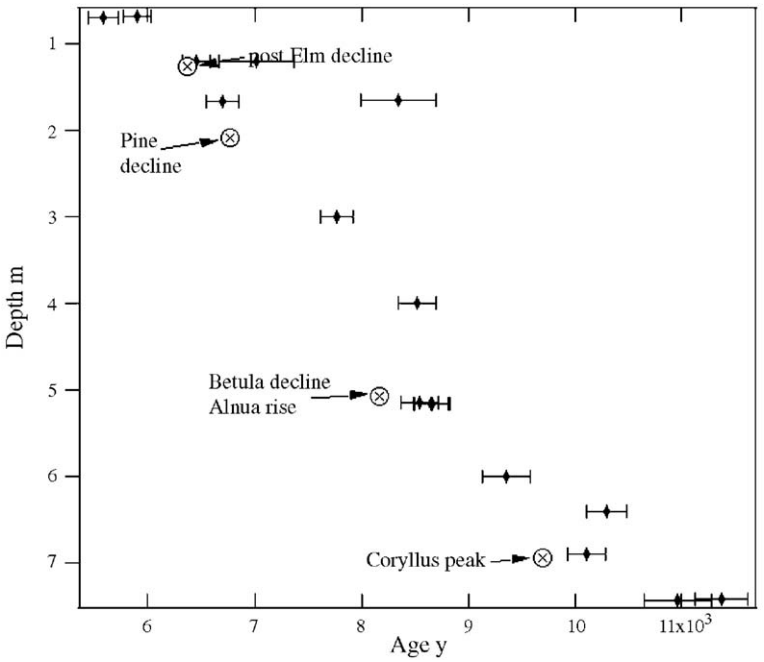

Fig. 4. Sampling depth in a sediment core of Hawes Water marls plotted against inferred ages for pollen marker horizons and U-series ages (with uncertainty), for authigenic sediment. Hawes Water, NW Lancashire, UK, is a small shallow lake and is much more responsive to climatic and hydrological change than large deep-water lakes, Marshall et al. (personal communication). The research focussed on the stable isotope and trace element record from ostracods and authigenic carbonate to reconstruct changes in temperature, hydrology and aquatic productivity. U-series ages match with a proxy chronology based on pollen horizons and stable isotopic data.

4.1.1. Inherited thorium

A disadvantage of marls is that they usually contain significant amounts of 'inherited' ^{230}Th from allogenic material. This can include detrital material such as carbonate or clay from the drainage area, or wind-blown dust (loess) or volcanic ash. It is a safe assumption that the allogenic material is in secular radioactive equilibrium and thus carries a significant amount of ^{230}Th. The effect of 'inherited' ^{230}Th on the overall calculated age of a sample depends on the age of the sample and on the uranium concentration. These effects can be illustrated with some simple calculations.

In this example, it is assumed that the authigenic phase has a U=1 μg g^{-1} and no thorium and the allogenic phase has 6.6 μg g^{-1} Th, a U/Th=0.238 and is in secular radioactive equilibrium. Ages can be calculated for assumed (^{230}Th/^{234}U) and (^{234}U/^{238}U) and a range of allogenic contributions by artificially increasing the thorium contribution. Results of such calculations are plotted in Fig. 5. For the oldest plotted age of 177 ka, the effect of 5 wt.% of allogenic contribution is a reduction in the calculated age of around 1%, comparable to the overall uncertainty of the age. However, the effect of only a 0.5 wt.% contribution of the same allogenic material is larger than the uncertainty for the 3 ka example. Higher thorium concentration in the allogenic contribution results in a roughly proportional reduction of the age. Recalculating the age effect for the 10 kyr sample but with an assumed Th=13.2 μg g^{-1} shows that with an allogenic contribution of 1.25 wt.%, the calculated age is 3.1% lower where with Th=6.6 μg g^{-1} the calculated age is 6.5% lower. Again, for younger samples the concentration effect is more pronounced than for the older samples.

Many other types of carbonate deposits, such as tufa and calcrete that are important in Earth and environmen-

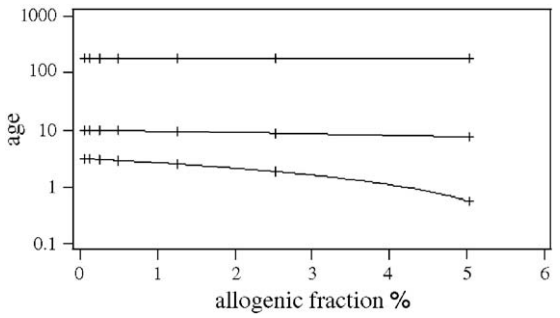

Fig. 5. Effect of 'inherited' ^{230}Th on the calculated age. In these model calculations for example, a 5 wt.% allogenic contribution has negligible effect on an age of 177 ka, but a 0.5 wt.% contribution is already resolvable on an age of 10 ka and would be significant on an age of 3 ka.

tal sciences also contain allogenic components, whereas corals and speleothem are usually less affected. Correct interpretation of U-series data requires that the effects of the allogenic contribution on ^{230}Th are adequately corrected. Three categories of approach can be distinguished: chemical separation, mathematical correction or empirical correction.

4.1.2. Chemical separation

The intention of chemical separation is to selectively dissolve the authigenic carbonate without attacking the other phases. The usual method is to use a weak mineral acid, or acetic or formic acid, or strong ligands, such as EDTA, that dissolve carbonate but not silicates. But even if the authigenic carbonate can be dissolved quantitatively without leaching the silicate (and that is doubtful given the nature and grain-size of the likely silicates), the dissolved authigenic ^{230}Th is highly particle-reactive and precipitates onto the silicate grains. Stronger reagents that would stabilise ^{230}Th in solution increase the likelihood of leaching of the allogenic phases. Moreover, even with mild reagents, it is impossible to completely avoid dissolving the almost invariable present detrital carbonate, resulting in a 'mixed age' that is always older than the true authigenic age. Small variations in the strength of the reagents, the duration of the reaction, the grain size and even the amount of material, all affect the selective dissolution process. Consequently, it is very difficult to obtain reproducible results using selective dissolution protocols.

4.1.3. Mathematical correction

Another way forward is mathematical modelling (Bischoff and Fitzpatrick, 1991; Luo and Ku, 1991). A number of samples of the same age (or very nearly so) but with different allogenic contributions are analysed. Data are plotted in activity diagrams such as (^{230}Th/^{232}Th) vs. (^{234}U/^{232}Th) and of (^{234}U/^{232}Th) vs. (^{238}U/^{232}Th). The slopes of best-fit lines through the data-points give (^{230}Th/^{234}U), and (^{234}U/^{238}U), respectively, and these are the input parameters for the classical Kaufman and Broecker (1965) age equation (Eq. (7)). The underlying assumption is that there is no ^{232}Th in the authigenic mineral and that all ^{232}Th is in one allogenic phase with a constant U/Th ratio in secular radioactive equilibrium. There are four different ways to arrange the relevant isotopes in ratios that can be used to calculate ages from either slope or intercept of best-fit lines, all giving equivalent results.

Ludwig (2003) and Ludwig and Titterington (1995) advocate fitting a plane through the (^{230}Th/^{238}U), (^{234}U/^{238}U) and (^{232}Th/^{238}U) data-points and this is usually referred to as the 'three-dimensional isochron approach'. However, the Kaufman and Broecker (1965) data evaluation method considers the samples to be a mixture of two phases, authigenic and allogenic, not a radioactively evolving closed system, as the use of the word 'isochron' implies. Ludwig and Titterington (1995) forms the basis for a regularly updated software package that is available from KR Ludwig and which has become the de-facto standard for calculating U-series ages and uncertainties.

Least-squares best-fit line routines are available in many spreadsheet software packages and give adequate answers for the two input parameters of Eq. (7).

Two independent factors have to be considered for uncertainty evaluation: analytical uncertainty and scatter of the data-points around the mixing lines. Total analytical uncertainty can be simply propagated by taking the square root of the sum of the squares of the individual uncertainties. Scatter of the data-points around the least-squares line is given by the minimised deviation. These two uncertainties can then be propagated to calculate an overall uncertainty estimate. In situations of simple two-component mixing of the authigenic material with variable amounts of one other component, the analytical uncertainty will dominate to total uncertainty. Where there is a limited range of mixing ratios, or variable proportions of more than one type of allogenic material, the uncertainty will be dominated by the scatter of the data-points around the mixing line.

In clean samples with a very limited allogenic contamination, the analytical uncertainty in the ^{232}Th contribution can become large, especially if the used analytical technique is alpha spectrometry, and can dominate the overall uncertainty unfairly. For such samples, it is adequate to simply subtract the small 'inherited' ^{230}Th contribution and ignore the uncertainty magnification.

4.1.4. Empirical correction

Another approach is the 'minimised standard deviation' method. This requires analysing the ^{232}Th concentration in the samples and assuming a Th/U ratio, such as a global average for shale, for the allogenic material, and secular radiogenic equilibrium. It is then simple to calculate the 'inherited' ^{230}Th and subtract the appropriate amount from the total ^{230}Th inventory. The assumed Th/U ratio that gives the lowest standard deviation in the calculated ages of a set of coeval samples, is the most appropriate. Analysis of the actual Th/U in the allogenic phase usually confirms the

empirical Th/U ratio and the average age is within the uncertainty of the age obtained with best-fit methods. For clean samples, the empirical correction would be preferable. The standard deviation of the ages is an acceptable estimate of the uncertainty on the average age. It is tempting to use the empirical Th/U to correct single samples from different horizons in the same sequence but the resulting calculated individual ages are then model-dependant and only analytical uncertainty should be reported.

4.2. Speleothem

Limestone deposits erode mainly by dissolution in carbonic acid forming from water that is charged with dissolved CO_2 derived from organic matter decay and soil respiration in vadose zones. Bacteriogenic sulphate may well be important for enlarging caves around underground water courses but the main agent for large-scale carbonate dissolution is carbonic acid. The partial pressure of CO_2 in vadose water is higher than the atmospheric equilibrium value and this allows an elevated concentration of calcium. Upon renewed contact of vadose water with atmosphere, excess CO_2 degasses, acidity decreases and $CaCO_3$ can precipitate. The result of this largely inorganic precipitation of calcite is called 'speleothem' (from the Greek for cave deposit) and it encompasses stalagmites, stalactites, flow stone tufa, and encrustations of objects, including fossils. Stalagmites, stalactites and flowstone form in caves, tufa forms at or near springs and encrustations in both.

4.2.1. Stalagmites

Stalactites are suspended from the cave ceiling and are rarely used for dating purposes because they are formed from variably degassed and degassing water and tend to be porous and 'open system' with respect to uranium. Stalagmites are usually considered the sample of choice because successive layers of calcite are neatly deposited on top of each other in the centre of a drip mound, from a well-defined drip point at the tip of a stalactite. Layers are also draped over the sides of the mound, usually still in an orderly fashion but mostly too thin for successful sampling for U-series dating. Stalagmites tend to be low in 'inherited' ^{230}Th from allogenic phases, and many characteristics such as morphometry, fluorescence index, trace element ratios and stable isotope ratios (hydrogen, carbon, oxygen, among others), including pollen (McGarry et al., submitted for publication), have been studied in a multi-proxy approach (McDermott, 2004; McDermott et al., in press; Fairchild et al., 2006-this issue; Fairchild et al., in press; Asrat et al., submitted for publication).

Stalagmites frequently show evidence of complicated growth history revealed by deposition hiatuses caused by changes in hydrological conditions as a consequence of climate variations such as dry periods or episode of glaciation. Other interruptions in the steady-state deposition regime are caused by cave flooding which results in detritus-rich layers. Deposition can also be interrupted by seismic activity that may even topple stalagmites. Sampling should be at a minimum on each side of each steady-state growth zone and this way the duration of any hiatus can be inferred.

On average, some 30 papers/yr exploiting speleothems are published, and some selected papers that use U-series dating of a paleo-environmental archive include the timing of sapropel formation in the Eastern Mediterranean, from analysis of speleothems in Soreq Cave, Israel (Bar-Matthews et al., 2000); paleo-environmental interpretation for late Middle Pleistocene speleothems, Victoria Fossil Cave, South Australia (Desmarchelier et al., 2000); millennial-scale climatic variability over the past 25,000 yrs in Southern Africa (Holmgren et al., 2003); 215 ka history of sea-level oscillations from marine and continental layers in Argentarola Cave speleothems, Italy, (Antonioli et al., 2004); Pleistocene climate variability from a stalactite, Nerja Cave, Spain (Jimenez de Cisneros et al., 2003); and climate oscillations during the last deglaciation from a speleothem from Tangshan Cave, China (Zhao et al., 2003).

An example of a paper that combines the use of environmental indicators and U-series dating was published by Genty et al. (2003). The authors correlate the terrestrial with the marine and ice-core age record to evaluate variations in $\delta^{18}O$ in a stalagmite, Vil9, the GISP ice core and MD95 sediment core. In Fig. 6, modified after Genty et al. (2003), numbers refer to Inter Stadials (e.g. Dansgaard et al., 1993). Vil9 stalagmite is from Villars Cave in the French Dordogne and data-points with uncertainty bars along the abscissa are U-series age determinations, D1–7 indicate discontinuities in the stalagmite. U-series dates on either side of visible discontinuities allow confident correlation of the $\delta^{18}O$ variations in the Villars stalagmite with the numbered warm stages recognised in the oceanic and ice-core records, which would not have been possible without dating. Note that only 3 of the 7 visually observed discontinuities result in a resolvable time hiatus and that D3 correlates with Heinrich event H6. Indirectly, these U-series dates contribute to the

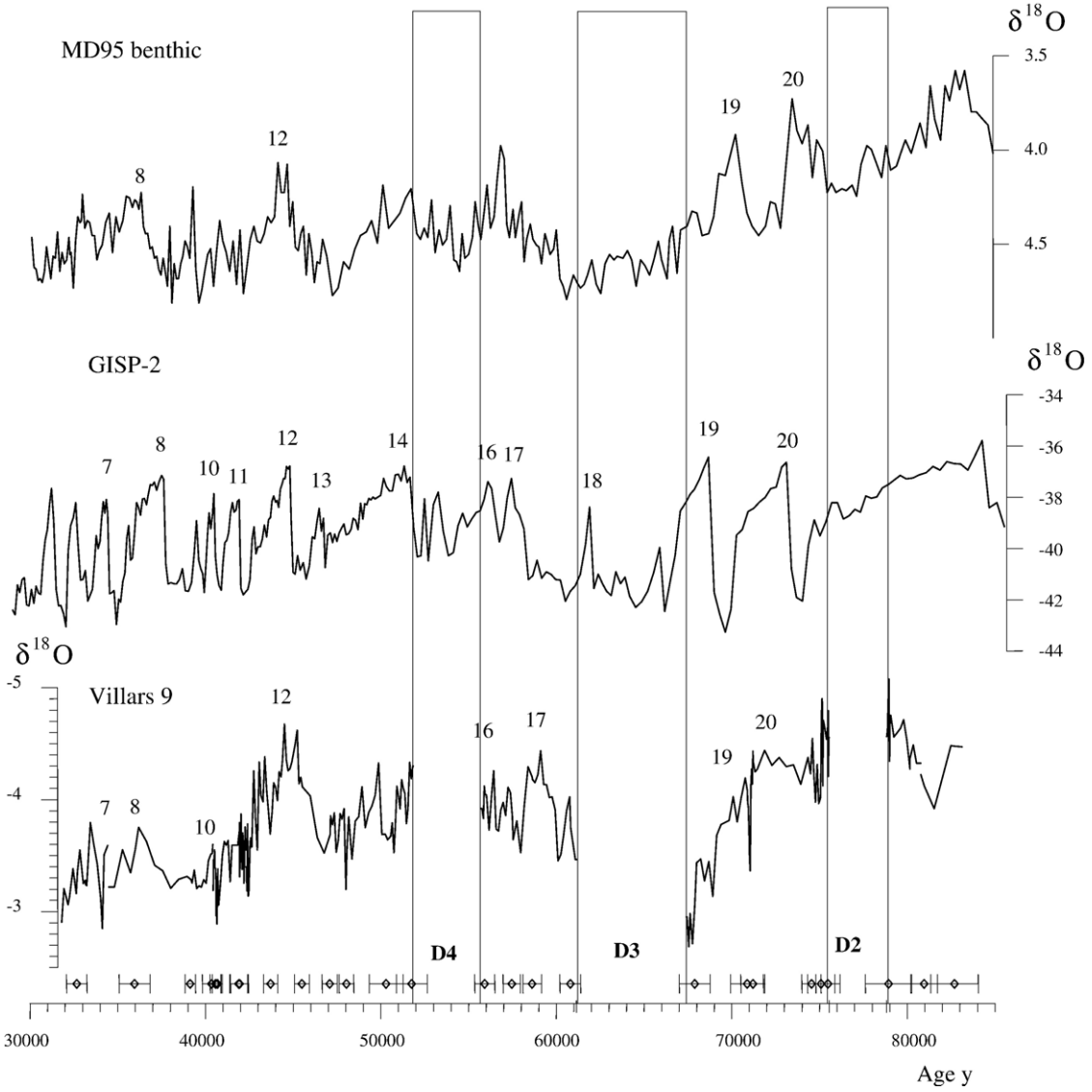

Fig. 6. Composite diagram, after Genty et al. (2003), showing variations in $\delta^{18}O$ in a stalagmite, Vil9, the GISP ice core and MD95 sediment core, numbers refer to Inter Stadials (e.g. Dansgaard et al., 1993). Data-points with uncertainty bars along the abscissa are U-series age determinations, D1–7 indicate discontinuities in the stalagmite. This stalagmite from Villars Cave in the French Dordogne is an example of the use of U-series dating in stalagmite-based paleo-climate research and is published in a recent paper by Genty et al. (2003). Stable isotope data, such as $\delta^{18}O$ and $\delta^{13}C$ that can be used as paleo-environment indicators, show a great deal of variation in this stalagmite. U-series dates on either side of visible discontinuities allow confident correlation of the $\delta^{18}O$ variations in the Villars stalagmite with the numbered warm stages recognised in the oceanic and ice-cap records, which would not have been possible without dating. Note that only 3 of the 7 observed discontinuities result in a resolvable hiatus and that D3 correlates with Heinrich event H6. Indirectly, these U-series dates contribute to the confidence in the dating of the ocean sediment and ice cores.

confidence in the dating of the ocean sediment and ice cores.

Despite the large number of U-series pin-points in Fig. 6, time between these pin-points still assumes a linear correlation with carbonate thickness and cannot be used to infer an accurate rate of temperature change during amelioration or cooling of individual warm stages. Temperature in the Dordogne during the Villars cold phase was probably more then 10C below current averages and permafrost would have been widespread in the area; see Genty et al. (2003) for a detailed discussion.

4.2.2. Flow stone and encrustations

Flow-stone deposits, also known as travertine, cover surfaces in caves where water flow from the ceiling and

walls is rather more equally distributed. Flow-stone can be clearly laminated, or form drapes that cover cave walls or can cement cave-earth or rubble or sometimes fossil bone, and appear more like a breccia (Latham, 1999).

Flow-stone usually incorporates relatively a large proportion of allogenic material but can yield age information if sufficiently clean material can be selected. Objects deposited on flow-stone tend to become covered with a carbonate crust deposited from ceiling drips. Where these objects are fauna or human fossils, they can be of great significance for paleo-ecology or paleo-anthropology and U-series dates of encrustations have been discussed by Latham and Schwarcz (1992).

U-series dates on flow-stone from one of the Zhoukoudian localities in China are marking the possible minimum age between 248 and 269 ka of a hominid fossil while samples taken from the lowest accessible strata date to ca. 300 ka, suggesting an even greater antiquity. These age assignment are broadly contemporaneous with the uppermost strata of the Peking Man site and support the hypothesis that human occupation of the Zhoukoudian sites has been more or less continuous over hundreds of thousand years (Shen et al., 2003).

4.3. Tufa

Around springs in limestone deposits, the same degassing of water that is rich in carbonic acid takes place and limestone deposits form. However, in tufa deposits, the calcite precipitation can be inorganic or mediated by the algae and microbes that flourish in the fresh, CO_2-rich water. The horizontal portions of tufa deposits from hanging springs are most favourable for U-series dating but these are the most difficult to interpret in an environmental framework because of the difficulty of horizontal correlations. Tufa is known as 'paludal' when it is deposited in a marsh environment and usually more extensive horizontally. Paludal tufa is rich in other environmental indicators but also in allogenic material (Garnett et al., 2004). Holocene pool and barrage tufa deposits are usually too rich in allogenic material but samples of freshwater travertine from Middle Velino Valley (Central Italy) have been successfully dated by Soligo et al. (2002) and used to infer paleoclimatic and geological implications. Eikenberg et al. (2001) have demonstrated the feasibility of combining U–Th with Th–Ra dating to achieve consistent dates that they have used to determine the geochemical evolution of travertine in the Hell Grottoes in Switzerland.

4.4. Caliche or calcrete

Calcrete deposits are similar to speleothems but here supersaturated ground-water percolates to the deposition zone at times when evaporation exceeds precipitation. Pedogenic calcrete deposits grow over time in a more-or-less orderly fashion where the earliest deposition occurs on the underside of the larger clasts. Calcite precipitates grow laterally, incorporating smaller clasts until eventually an indurated zone is formed. The indurated zone or 'pan' interrupts percolation and effectively halts calcite deposition although finely laminated calcite may still be deposited on top of the pan, sometimes specifically around roots. Calcrete crusts vary in thickness from centimeters to many meters and at deposition rates of generally <0.1 mm/yr, it takes tens of thousands of years to form meter-thick deposits. Calcrete deposition depends on local physiographic and climate conditions and the potential of calcrete as an indicator of landscape evolution and as a climate archive depends accurate dating.

Recent papers by Candy et al. (2005a,b) demonstrate the application of U-series data, to estimate the rate and sequence of calcite deposition from the earliest coatings on the underside of clasts to the last deposit on top of the pan. They describe sampling of carbonate from within a mature (stage V) pedogenic calcrete profile from southeast Spain. The locations of the earliest and latest cements were estimated from calcrete morphological development with micro-morphological analysis of the profile. Carbonate was sampled and dated from three locations within the profile: below the lower surface of clasts within the hardpan (the earliest cement), from the centre of cement-filled pores within the hardpan (the final phase of hardpan permeability) and from the laminar calcrete overlying the hardpan (post-hardpan cement).

U-series results show that the carbonate below the lower surface of the clasts formed at 207 ± 11 ka, the carbonate from within the in-filled pores formed 155 ± 9 ka and the laminar crust formed 112 ± 15 ka.

Taking into consideration the associated uncertainties, it can be deduced that between 72 and 32 kyr were required for the hardpan calcrete to form. The laminar calcrete formation continued 19 to 77 kyr on top of the hardpan calcrete. This is the first time that rates of mature calcrete development have been established by direct radiometric dating of the authigenic carbonate. The technique is appropriate for dating mature calcretes in arid regions worldwide and offers the opportunity of increasing our understanding of the spatial and temporal variability in rates of pedogenic calcrete development.

Calcrete invariably contains allogenic material but usually sufficiently clean material for analysis can be obtained by drilling from hand specimen in the laboratory. Nevertheless, multiple coeval samples should be analysed to be able to construct mixing lines or isochrons. Candy et al. (2005b) used the 'three-dimensional isochron approach' (Ludwig and Titterington, 1995) to calculate ages. Using a least-squares best-fit routine to calculate mixing lines through the data-points to determine the input ratios for the Kaufman and Broecker (1965) equation the ages would be 215 ± 9 ka (isochron = 207 ± 11), 154 ± 4 ka (isochron = 155 ± 9), 111 ± 13 ka (isochron = 112 ± 15), all uncertainties are 2 S.D. Candy et al. (2005b) used 11, 10 and 12 samples, respectively, to obtain the range in isotope ratios to compute the calcrete ages.

4.5. Organically mediated carbonate deposits

For many organisms the organ-support structure consists of calcite or aragonite that has been precipitated with the aid of enzymes. There is a long list of such organisms that ranges from plants to animals and from simple to evolved. For the purpose of this discussion, we will consider carbonates where the U/Ca ratio reflects that ratio in the water as 'simple' and those organisms that more or less effectively reduce the uranium concentration as 'evolved'. Most observations relate to seawater but probably apply equally to freshwater organisms.

4.5.1. Simple organisms

It would appear that 'simple' organisms are easier to date because these have relatively high uranium concentration, in the low μg g^{-1} range for corals and foraminifera. However, 'simple' coral and indeed forams can have a very delicate structure and diffusion distances across thin septa are very short. Moreover, degradation of inter-crystalline organic material increases porosity and uranium can be quite easily leached by rainwater from exposed coral. The extent of leaching can be assessed by simple modelling.

A number of checks can be carried out on coral samples to evaluate the suitability for U-series dating. Visual and microscopic inspection is carried out to assess the absence of detritus, and X-ray analysis is useful to ascertain absence of re-crystallisation. After initial selection and sample analysis, it is usually assumed that if the ($^{234}U/^{238}U$) in the carbonate is the same as in the surrounding seawater, the system has remained 'closed' (Henderson, 2002) and samples with deviation values are considered as suspect. The accepted ($^{234}U/^{238}U$) value for seawater is 1.145 ± 2‰ and this value has remained constant for at least the past 800 kyr (Henderson, 2002) in the open ocean. However, ($^{234}U/^{238}U$) may be different in restricted basins with reduced salinity or with hydrothermal input. The same criteria can be applied to foraminifera and these have also been used to great effect (Robinson et al., 2002).

Despite careful selection, some samples still do not conform to expectations and yield unexpected ages, and others that were rejected based on deviating ($^{234}U/^{238}U$) values, give perfectly acceptable ages (Gallup et al., 1995; Stirling et al., 1995). This aberrant behaviour is sometimes blamed on early diagenesis and we will return to this later. Recently, ^{235}U–^{231}Pa systematics has been applied to coral dating (Mortlock et al., 2005; Edwards et al., 1997), as a confirmation of ^{234}U–^{230}Th ages. Good agreement has been observed despite the relatively difficult ^{231}Pa quantification.

4.5.2. Evolved organisms

Gastropods and molluscs have always been considered as difficult to date by U-series methods since Kaufman et al. (1971) found that approximately half of the analysed samples yielded ages that did not fit in with established chronologies. However, molluscs such as Cardium and Anadonta, have been successfully dated recently with U-series methodology (Petit-Maire et al., 2002; Arslanov et al., 2002, respectively). The previously encountered difficulties can be partly explained by the relatively low initial U/Ca and uranium concentration in gastropod and mollusc shells which leads to uranium absorption from seawater after death. Uranium uptake from vadose water after emergence is also possible. The absorption process is as yet not well understood but unlikely to be homogeneous, given the variations in thickness, density and porosity in many shells.

Holocene marine mollusc shells have been dated using $^{226}Ra/Ba$ ratios. In clean shells, ^{226}Ra concentrations and $^{226}Ra/Ba$ ratios show a clear decrease with increasing age, suggesting the possibility of ^{226}Ra dating. Limiting factors for dating are Ba and ^{226}Ra in surface contaminants, and in-growth of ^{226}Ra from U present within the shell. Moderate levels of contamination can be corrected by using sub-samples from the same shell with different proportions of contamination to form a mixing line in a $^{226}Ra/Ba$–$^{232}Th/Ba$ space. ^{226}Ra in-growth from U within the shell is important only when ages exceed ~2500 yrs. Calculated ages are similar to those expected from simple ^{226}Ra excess decay

from seawater ^{226}Ra/Ba values. In younger shells, ^{226}Ra/Ba ratios corrected for surface contamination provide chronological information, (Staubwasser et al., 2004).

5. Uranium loss

In common with other isotope systems, and relevant to all U-series systems discussed so far, understanding open system behaviour, i.e., the uptake or loss of parent or daughter isotopes from the system, is essential for appropriate interpretation of the data. The 'loss' process can be viewed as a diffusion process and the parameters are temperature, time, diffusion coefficient, concentration contrast and the diffusion distance. Diffusion processes are crucially important for radiogenic isotope systems at higher temperatures where the effective cessation of diffusion marks the 'closure temperature' of the system and is the 'event' that is most commonly dated. However, at environmental temperature and in solid state, diffusion coefficients are so low that time is insufficient and the system remains 'closed'. Diffusion where one of the phases is a mobile fluid typically have a very large concentration contrast but since the mobile fluid phase is usually water, dissolution–precipitation processes are orders of magnitude faster than solid-state diffusion of trace elements. Selective or partial dissolution are the relevant 'open system' processes for U-series systematics at environmental conditions.

5.1. Dissolution

The main process that drives trace-element loss is focussed dissolution of the mineral phase. Water permeates along grain boundaries and micro-cracks (sometimes these cracks are formed by re-crystallisation of aragonite to calcite) and removes, or replaces atoms from the grain and sub-grain surface layers. Dissolution may be selective and trace elements such as uranium can be removed faster than the major elements of the mineral.

5.2. Recoil

In a U-series context there is the added complication usually referred to as 'α-recoil'. The term derives from physics where it describes the displacement of a radiogenic daughter isotope in the crystal lattice, when the radioactive parent nuclide has experienced a decay reaction. The displacement is not trivial, 10–110 nm for ^{238}U to ^{234}Th and it leaves a tube in the crystal of that length. Further β-decay of ^{234}Th to ^{234}U has little effect because the kinetic energy of β-decay is much smaller than α-decay. If uranium is not homogeneously distributed throughout the sample then the effect of ^{234}U displacement is that U-rich domains will evolve to $(^{234}U/^{238}U) < 1$ and the opposite for U-poor domains. A recoil track that intersects the grain surface provides an easy path for the decayed atom to move through. In effect, recoil creates a thin layer with enhanced permeability. However, the α-recoil effect only affects daughter isotopes such as ^{234}Th and its daughter ^{234}U and not the ^{238}U because ^{238}U is not radiogenic. Permeability is selectively enhanced for the ^{234}U daughter isotope and the leaching process results in *non-mass dependent* isotope fractionation where the solid phase is depleted in $(^{234}U/^{238}U)$ and the liquid phase is enriched. The extent of non-mass dependant isotope fractionation depends on the extent of the total surface layer with α-recoil enhanced permeability and is therefore dependent on the grain-size distribution of the material in contact with water.

One important consequence of $(^{234}U/^{238}U)$ fractionation by the recoil process is that this ratio in water can be very different from the secular equilibrium value. $(^{234}U/^{238}U)$ can be very high, e.g. values as high as 6 have been reported (Reynolds et al., 2003).

5.2.1. Simple modelling

It is instructive to model some of the consequences of ^{234}U mobility as a consequence of α-recoil using the equations derived by Henderson et al. (1999). The secular equilibrium value of $(^{234}U/^{238}U)$ in pore water depends largely on the grain size of the matrix and the matrix to pore–volume ratio and is given by:

$$\left(\frac{^{234}U}{^{238}U}\right)_{sec-eq} = \frac{r^3-(r-\alpha)^3}{4r^3} \times \frac{^{238}U_{matrix}}{^{238}U_{pore}} \times \frac{\rho_{matrix}}{\rho_{pore}} \times \frac{(1-\phi)}{\phi} + 1 \quad (8)$$

where r is the grain size radius, α is the α-recoil distance, ρ is the density and ϕ is the porosity and other symbols as before.

The approach of $(^{234}U/^{238}U)$ to the equilibrium value calculated with Eq. (8) is given by:

$$\left(\frac{^{234}U}{^{238}U}\right)_t = \left\{\left(\frac{^{234}U}{^{238}U}\right)_{sec-eq} - \left(\frac{^{234}U}{^{238}U}\right)_{init}\right\} \times \left\{1-e^{-t\lambda_{234}}\right\} + \left(\frac{^{234}U}{^{238}U}\right)_{init} \quad (9)$$

As a simple example we assume a situation of seawater-derived pore water that is stagnant in a matrix of grains and that the grain-size is homogeneous rather

than a distribution. Also assuming U=3 μg g^{-1} in the grains and U=3 ng g^{-1} in seawater and an average recoil length of 55 nm.

The ($^{234}U/^{238}U$) in the pore water depends on two processes, radioactive decay, from ($^{234}U/^{238}U$)=1.145 in seawater to the equilibrium value ($^{234}U/^{238}U$)=1, and the preferential addition of ^{234}U from the α-recoil zone, and can be calculated with Eq. (8). The rate of increase of ($^{234}U/^{238}U$) depends on the total area of the enhanced permeability grain surface layer that is in contact with the pore-water, and therefore on the grain-size, and the effect is quite marked. The equilibrium ($^{234}U/^{238}U$) in static pore water is >100 at 0.6 μm and almost 40 at 2 μm. But at larger than 0.6 mm, decay dominates and ($^{234}U/^{238}U$) approaches a value of 1 after five half-lives of ^{234}U. The rate at which the equilibrium value is approached can be calculated with Eq. (9) and equilibrium is achieved fairly rapidly with small grain sizes, 30 yrs for 0.6 μm and 100 yrs for 2 μm. Fig. 7a–b illustrate some results of these model calculations.

Even from these simplistic calculations some interesting inferences could be made about differences in ($^{234}U/^{238}U$) between seawater and authigenic carbonate, accepting that the assumptions are reasonably realistic.

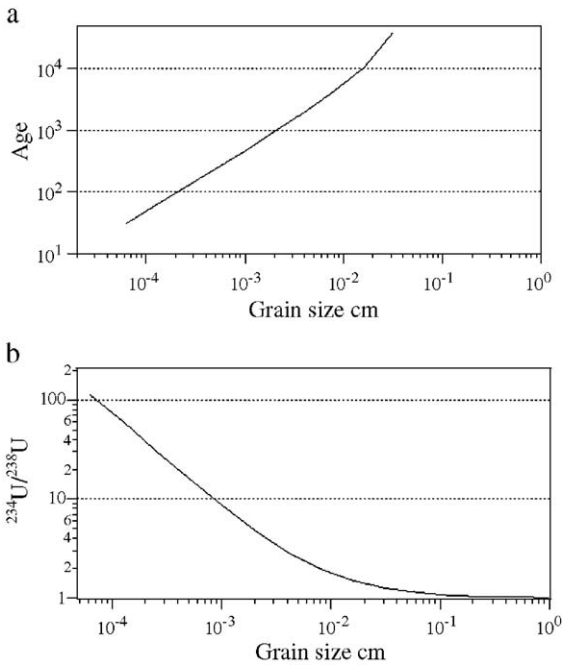

Fig. 7. (a) The effect of grain-size variation on the equilibrium value of ($^{234}U/^{238}U$), calculated with Eq. (8), assuming 3 μg g^{-1} uranium concentration in the grains, 3 ng g^{-1} uranium concentration in the stagnant pore water, 55 nm average recoil-track length and homogeneous grain size. (b) The effect of grain-size variation on the time required to attain ($^{234}U/^{238}U$) equilibrium calculated with Eq. (9), same assumptions as panel (a).

At a seafloor sediment precipitation rate of 1 cm/1000 yrs with the average grain size in the normal range for pelagic clay, ($^{234}U/^{238}U$) in the pore water will deviate significantly from the seawater value after seawater percolation ceases, within the life-span of many sessile organisms. Based on data for NE Atlantic deep-sea sediments Thomson et al. (submitted for publication) argue that bioturbation causes mixing of the top 12 cm of sediment and, based on ^{14}C arguments that the average age of the homogenised layer is of the order of 2000 yrs for an average sedimentation rate of 4–7 cm/kyr. The averaged ($^{234}U/^{238}U$) of pore water depends on the grain size distribution of the mixed sediment but for grain-sizes <40 μm, the ($^{234}U/^{238}U$) will be >3. Authigenic carbonate precipitate in the mixed layer is unlikely to have a seawater ($^{234}U/^{238}U$) value. Continental shelf sediments tend to accumulate intermittently allowing more time for ($^{234}U/^{238}U$) evolution, and it should be expected that neither authigenic precipitates nor subsurface feeders have seawater ($^{234}U/^{238}U$) values in this situation.

It is still a reasonable assumption that plankton and coral which feed by filtering seawater and extract the ions required for building a calcite skeleton from seawater, should have seawater ($^{234}U/^{238}U$) values. Buried molluscs and gastropods that live in or on the sediment surface and feed by processing detritus are unlikely to maintain seawater ($^{234}U/^{238}U$) ratios.

For carbonate that has been precipitated within ocean water it is reasonable to expect that the ($^{234}U/^{238}U$) value is within analytical uncertainty of the seawater value but the ($^{234}U/^{238}U$) ratio within sediment can change rapidly, depending on grain size distribution and pore water flow. By implication, the ($^{234}U/^{238}U$) ratio in detritus feeders could very well be above seawater values.

5.2.2. Recoil modelling

Two important observations regarding α-recoil have been made by Henderson et al. (2001) and Villemant and Feuillet (2003). These authors have highlighted the fact that both ^{238}U and ^{234}U decay to thorium isotopes, ^{234}Th with a half-life of 24 days and ^{230}Th with a half-life of 75 kyr, respectively. They have also pointed out that α-recoil damage accumulates with time and is directly related to the radioactive decay of the parent nuclides. The α-recoil damage to the mineral lattice from both α-decay processes depends on the energy of the α-recoil reactions, which is determined for a given mineral by the nuclear reaction characteristics

and is very similar for both nuclides. The similarity of both ^{238}U and ^{234}U recoil processes allows them to be coupled and U-series data can be modelled assuming that α-recoil is the only other process that affects isotope ratios, as well as radioactive decay. The equations that describe the combined processes of radioactive decay and recoil are essentially an expansion of the Kaufman and Broecker (1965) equation with an '*f*' factor for each of the recoil reactions and maintaining a fixed relation between the two '*f*' factors. The '*f*' factor represents the fraction of daughter isotope lost or gained and can be seen as the 'open system' factor.

The Villemant and Feuillet (2003) model can explain the scatter in U-series data for various Quaternary marine terraces and uses a simplified inversion procedure for the calculation of the ages of these terraces. The Villemant and Feuillet (2003) model also allows for the input of inherited ^{230}Th but crucially assumes that the initial ($^{234}U/^{238}U$) is known. ($^{234}U/^{238}U$) is 1.145 for precipitation of uranium in equilibrium with seawater in the open ocean. However, as indicated in the simple model calculations above (Section 5.2.1), interaction with pore-water uranium during early diagenesis can result in evolving ($^{234}U/^{238}U$). Moreover, there are many other situations where ($^{234}U/^{238}U$) is not known such as in marginal or hydrothermally affected sea areas. In cases where equilibrium ($^{234}U/^{238}U$) from pore-water analysis is not available, ($^{234}U/^{238}U$) is actually a free parameter. Fig. 8 is a ($^{234}U/^{238}U$) vs. ($^{230}Th/^{234}U$) diagram with five, nearly straight isochron curves and four evolution curves for different degrees of open-system behaviour with the closed-system curve indicated by $f=1$. Data-points (black squares) are for four carbonate samples from Lake Tswaing (Thorpe et al., 2005). Lake Tswaing is an intra-continental aquifer-fed hyper-saline closed lake in a depression formed by a meteorite impact and the four data-points define an age of 165 ka, after correction for a small allogenic contribution. In Fig. 8 the data-points plot near a 165 ka isochron for ($^{234}U/^{238}U$)=2.85 and then indicate '*f*' values of 0.8–0.9 and negligible allogenic ^{230}Th, inferred from a low $^{230}Th/^{234}U$ initial value at zero age. The distribution of data-points along isotope ratio evolution curves indicates that a small amount of ^{234}U loss, inferred from an open system factor '*f*' of within 15% of the closed system value of unity still given valid U-series ages, as was also observed by Villemant and Feuillet (2003) for Quaternary marine terraces. The inferred ($^{234}U/^{238}U$)=2.85 is within expectations for carbonate that has precipitated from phreatic water that slowly percolated through an aquifer.

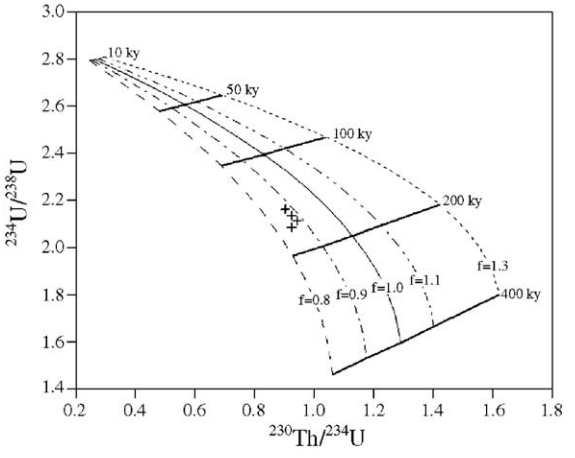

Fig. 8. ($^{234}U/^{238}U$) vs. ($^{230}Th/^{234}U$) diagram. Solid, nearly straight curves are isochrons, evolution curves for different degrees of open-system behaviour as indicated by the '*f*' values, are broken lines with the closed-system solid curve indicated by $f=1$. Curves and isochrones are calculated with the equations in Villemant and Feuillet (2003). The initial value for ($^{230}Th/^{234}U$), indicating the allogenic contribution, is very low; the initial value for ($^{234}U/^{238}U$) may indicate the ambient ratio during precipitation but is essentially unconstrained.

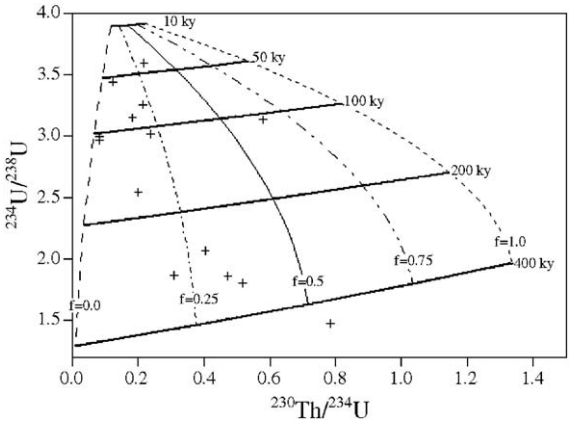

Fig. 9. ($^{234}U/^{238}U$) vs. ($^{230}Th/^{234}U$) diagram. Solid, nearly straight curves are isochrons, evolution curves for different degrees of open-system behaviour as indicated by the '*f*' values, are broken lines the evolution curve marked 0 is for systematic loss of all uranium isotopes. Closed-system is indicated by the dashed curve for $f=1$.

In a situation where the equilibrium ($^{234}U/^{238}U$) can be constrained either by assuming equilibrium with a seawater value or by data from pore-water analysis, an age can be calculated. Conversely, ($^{234}U/^{238}U$) can be inferred with the Villemant and Feuillet (2003) model if the age can be independently constrained.

The ($^{234}U/^{238}U$) vs. ($^{230}Th/^{234}U$) diagram can also be used to indicate an open system situation if data-points plot $0.8>f>0$ where $f=0$ indicates systematic ^{234}U and ^{238}U loss. Fig. 9 is a ($^{234}U/^{238}U$) vs.

(^{230}Th/^{234}U) diagram similar to Fig. 8 but the data-points are from a section of finely laminated lake sediments of Laguna Piuray, Peru (M. Burns and B. Aston, personal communication, 2005). The carbonate sediments are probably post-glacial and became exposed when a moraine dam eroded. It can be concluded from the scattering of the data-points over the diagram that exposure to rain and groundwater percolation resulted in extensive disruption to the U-series system. Data-points close to the $f=0$ evolution curve indicate almost total loss of all uranium isotopes. In this case, the Villemant and Feuillet (2003) model can be used to argue that it is unlikely that age information may be recovered from these data.

6. Uranium uptake in bone

Uranium concentration in bone–apatite structure of living animals and humans is very low, a small fraction of a μg g^{-1}, but the capacity of bone to adsorb uranium is phenomenal, many hundreds of μg g^{-1} has been measured. Large amounts of uranium can be absorbed, most probably from phreatic water. Millard and Hedges (1996) developed a uranium uptake model, known as the diffusion and adsorption or D/A model, based on a physico-chemical description of uranium–bone interaction.

With the D/A model the uranium distribution in bone can be calculated, assuming that ground-water flows through the bone pore-space by a process similar to diffusion and uranium is immobilised on to the large surface area of the fine-grained, hydroxyl-apatite by a process similar to adsorption. At the core of this model is the parameter D/R which is a function of the diffusion coefficient and the adsorption coefficient of uranium for bone. D/R is related to the structure of the bone and therefore quite different in tooth material, but D/R is also dependent on the hydrology of the burial environment.

The D/A model not only predicts the rate of uranium uptake, but also the spatial distribution of uranium within a bone. In a bone cross section, the uranium concentration distribution should approximate two diffusion profiles, mirrored in the centre, resulting in a ∪-shape. With time, the centre of the ∪-shape will become shallower and, in equilibrium, the profile will be a horizontal line over the top of the ∪-shape.

Pike et al. (2002) have developed the diffusion–adsorption model to incorporate U-series disequilibrium to dating of bone. The U-D/A model predicts the development of uranium and thorium isotope ratios across a bone section, as closed system U-series ages. For a given value of the D/R parameter, closed system ages across a bone form a ∪-shaped pattern with a pronounced valley and a flat bottom for very young ages. Older patterns become more shallow ∪-shaped and equilibrium ages are characterised by a horizontal pattern.

The uranium concentration distribution across a bone section is used with the D/A model to estimate the D/R parameter which is then an input parameter for the U-D/A model. U-profiles are calculated for various ages and the pattern with the lowest least-squares deviation gives the best estimate for the age of the bone. The least-squares deviation is a reasonable estimate of the uncertainty of the ages because it is based on a number of samples, usually a minimum of 5, and is always in excess of the analytical uncertainty. It is worth noting that the maximum ages that can be calculated with the U-D/A model is higher than commonly stated maximum of 5 half-lives of ^{230}Th or 380 kyr, depending on the time-scale of the diffusion process.

Pike et al. (2005) have applied the U-D/A model to Late Pleistocene mammalian bones from Wood Quarry in Nottinghamshire UK, see Fig. 10. Because seven individual U-series dates from one bone conform to a U-D/A model age that makes sense in a wider context, it is fair to state that such ages can be considered as quite robust. The weighted mean of four bone samples is quoted as 66.8 ± 3.0 ka, within or just before Marine Oxygen Isotope Stage 5. This age allows correlation with the Banwell Bone Cove fauna in Somerset which precedes the mammalian assemblage from nearby (<5 km) Creswell Crag caves.

The U-D/A model indicates that previously used mathematical descriptions for uranium uptake, such as

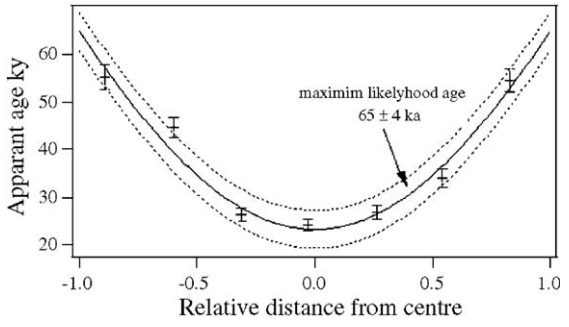

Fig. 10. The U-D/A model applied to Late Pleistocene mammalian bones from Wood Quarry in Nottinghamshire UK, after Pike et al. (2005). Individual U-series ages are based on 'closed system' assumptions for 7 sub-samples across a section of mammalian bone. The curve is the 'best fit' U-D/A model curve through these data-points and corresponds to an age of 65 ± 5 ka where the uncertainty reflects the distribution of the data-points around the model curve.

constant uptake over time, or instant uptake after burial, are too simplistic. However, the U-D/A model is only successful if the hydrological conditions at the burial site remain constant and the uranium concentration in the ground-water is constant. Less than ideal conditions manifest themselves as deviations from the model ∪-shape of both uranium concentrations and U-series closed-system ages. Such patterns can be modelled but require a larger number of assumptions.

7. Conclusions

U-series methodology can be used in environmental research and science-based archaeology as well as in geological research into magma chamber evolution and volcanic hazard prediction, e.g.: Macdougall (1995).

The ^{238}U–^{234}U–^{230}Th–^{226}Ra system with half-lives of 245 kyr, 76 kyr and 1.6 kyr, respectively, covers the time-scales of many environmental processes but is most suitable for processes that leave solid evidence in the form of authigenic mineral phases in deposits that also record significant environmental parameters or their proxies. U-series methodology depends on the efficient separation of uranium and thorium in environmental processes. Open-system behaviour, 'inherited' ^{230}Th, and uranium loss, can all result in erroneous conclusions but it has been shown that mathematical correction models can be used to recover information in many cases.

Acknowledgements

Reviews by S Black, R Parrish and P Rowe are much appreciated.

References

Antonioli, F., Bard, E., Potter, E.-K., Silenzi, S., Improta, S., 2004. 215-ka History of sea-level oscillations from marine and continental layers in Argentarola Cave speleothems (Italy). Global and Planetary Change 43, 57–78.

Arslanov, Kh.A., Tertychny, N.I., Kuznetsov, V.Yu., Chernov, S.B., Lokshin, N.V., Gerasimova, S.A., Maksikov, F.E., Dodonov, A.E., 2002. $^{230}Th/U$ and ^{14}C dating of mollusc shells from the coast of the Caspian, Barents, White and Black Seas. Geochronometria 21, 49–56.

Asrat, A., Baker, A., Umer, M., Moss, J., Leng, M., Calsteren P. van, Smith, C., submitted for publication. A high-resolution multi-proxy stalagmite record from Mechara, Southeastern Ethiopia: Paleohydrological implications for speleothem paleoclimate reconstruction.

Bar-Matthews, M., Ayalon, A., Kaufman, A., 2000. Timing and hydrological conditions of Sapropel events in the Eastern Mediterranean, as evident from speleothems, Soreq cave, Israel. Chemical Geology 169, 145–156.

Bischoff, J.L., Fitzpatrick, J.A., 1991. U-series dating of impure carbonates: an isochron technique using total-sample dissolution. Geochimica et Cosmochimica Acta 55 (2), 553–555.

Blake, S., Rogers, N.W., 2005. Magma differentiation rates from $(^{226}Ra)/(^{230}Th)$ and the size and power output of magma chambers. Earth and Planetary Science Letters 236 (3–4), 654–669.

Bourdon, B., Turner, S., Henderson, G.M., Lundstrom, C.C. (Eds.), 2005. Applications of U-Series methodology, Reviews in Minera logy and Geochemistry, vol. 52.

Calsteren, P., van Schwieters, J.B., 1995. Performance of a thermal ionisation mass spectrometer with a deceleration lens system and post-deceleration detector selection. International Journal of Mass Spectrometry and Ion Processes 146/147, 119–129.

Candy, I., Black, S., Sellwood, B.W., 2005a. Quantifying time scales of pedogenic calcrete formation using U-series disequilibria. Sedimentary Geology 170, 177–187.

Candy, I., Black, S., Sellwood, B.W., 2005b. U-series isochron dating of immature and mature calcretes as a basis for constructing Quaternary landform chronologies for the Sorbas basin, southeast Spain. Quaternary Research 64 (1), 100–111.

Chen, J.H., Edwards, R.L., Wasserburg, G.J., 1986. ^{238}U, ^{234}U and ^{232}Th in seawater. Earth and Planetary Science Letters 80, 241–251.

Cochran, J.K., Carey, A., Sholkovitz, E.R., Surprenant, L.D., 1986. The geochemistry of uranium and thorium in coastal marine sediments and sediment pore waters. Geochimica et Cosmochimica Acta 50 (5), 663–680.

Dansgaard, W., Johnson, S.J., Clausen, H.B., Dahl-Jensen, D., Gundestrup, N.S., Hammer, C.U., Hvidbjerg, C.S., Steffensen, J.P., Sveinbjörnsdottir, A.E., Jouzel, J., Bond, G., 1993. Evidence for general instability of past climate from a 250-kyr ice-core record. Nature 364, 218–220.

Desmarchelier, J.M., Goede, A., Ayliffe, L.K., McCulloch, M.T., Moriarty, K., 2000. Stable isotope record and its palaeoenvironmental interpretation for a late Middle Pleistocene speleothem from Victoria Fossil Cave, Naracoorte, South Australia. Quaternary Science Reviews 19, 763–774.

Edwards, Lawrence, R., Chen, J.H., Ku, T.-L., Wasserburg, G.J., 1987. Precise timing of the last interglacial period from mass spectrometric determination of Thorium-230 in corals. Science 236, 1547–1553.

Edwards, R.L., Cheng, H., Murrell, M.T., Goldstein, S.J., 1997. Protactinium-231 dating of carbonate by thermal ionisation mass spectrometry: implications for Quaternary climatic change. Science 276, 782–786.

Eikenberg, J., Vezzu, G., Zumsteg, I., Bajo, S., Ruethi, M., Wyssling, G., 2001. Precise two chronometer dating of Pleistocene travertine: the $^{230}Th/^{234}U$ and $^{226}Ra_{ex}/^{226}Ra_{(0)}$ approach. Quaternary Science Reviews 20, 1935–1953.

Fairchild, I.J., Smith, L.C., Baker, A., Fuller, L., Spotl, C., Mattey, D., McDermott, F., EIMF, 2006. Modification and preservation of environmental signals in speleothems. Earth-Science Reviews 75, 105–153. doi:10.1016/j.earscirev.2005.08.003 (this issue).

Fairchild, I.J, Frisia, S., Borsato, A., Tooth, A.F., in press. Speleothems in their geomorphic, hydrogeological and climatological context. In: Nash, D. J., McLaren, S.J. (Eds). Geochemical Sediments and Landscapes, Blackwells, Oxford.

Gallup, C.D., Edwards, R.L., Johnson, R.G., 1995. The timing of high sea levels over the past 200,000 years. Science 263 (5158), 796–800.

Garnett, E.R., Gilmour, M.A., Rowe, P.J., Andrews, J.E., Preece, R.C., 2004. Th-230/U-235 dating of Holocene tufas: possibilities and problems. Quaternary Science. Reviews 23 (7–8), 957–958.

Genty, D., Blamart, D., Ouahdi, R., Gilmour, M., Baker, A., Jouzel, J., Van-Exter, S., 2003. Precise dating of Dansgaard–Oeschger climate oscillations in western Europe from stalagmite data. Nature 521 (6925), 833–837.

Grimes, S., Rickard, D., Hawkesworth, C., van Calsteren, P., Browne, P., 1998. A U–Th calcite isochron age from an active geothermal field in New Zealand. Journal of Volcanology and Geothermal Research 81 (3–5), 327–333.

Henderson, G.M., 2002. Seawater (U-235/U-238) during the last 800 thousand years. Earth and Planetary Science Letters 199 (1–2), 97–110.

Henderson, G.M., Burton, K.W., 1999. Using ($^{235}U/^{238}U$) to assess diffusion rates of isotope tracers in ferromanganese crusts. Earth and Planetary Science Letters 170, 169–179.

Henderson, G.M., Slowey, N.C., Haddad, G.A., 1999. Fluid flow through carbonate platforms: constraints from $^{235}U/^{238}U$ and Cl^- in Bahamas pore-waters. Earth and Planetary Science Letters 169 (1–2), 99–111.

Henderson, G.M., Slowey, N.C., Fleisher, M.Q., 2001. U–Th dating of carbonate platform and slope sediments. Geochimica et Cosmochimica Acta 65 (16), 2757–2770.

Holmgren, K., Lee-Thorp, J.A., Cooper, G.R.J., Lundblad, K., Partridge, T.C., Scotte, L., Sithaldeen, R., Talmaf, A.S., Peter, D., Tyson, P.D., 2003. Persistent millennial-scale climatic variability over the past 25,000 years in Southern Africa. Quaternary Science Reviews 22, 2311–2326.

Israelson, C., Bjorck, B., Hawkesworth, C.J., Noe-Nygaard, N., 1998. Uranium-series isotopes from Eemian lake deposits, Hollerup, Denmark. Bulletin of the Geological Society of Denmark 44, 173–179.

Ivanovich, M., Harmon, R.S. (Eds.), 1982. Uranium Series Disequilibrium Applications to Environmental Problems. Oxford University, Press.

Jimenez de Cisneros, C., Caballero, E., Vera, J.A., Duran, J.J., Julia, R., 2003. A record of Pleistocene climate from a stalactite, Nerja Cave, southern Spain. Palaeogeography, Palaeoclimatology, Palaeoecology 189, 1–10.

Kaufman, A., Broecker, W.S., 1965. Comparison of ^{230}Th and ^{14}C ages for carbonate materials from Lakes Lahontan and Bonneville. Journal of Geophysical Research 70, 4039–4054.

Kaufman, A., Broecker, W.S., Ku, T.-L., Thurber, D.L., 1971. The status of U-series methods of mollusc dating. Geochimica et Cosmochimica Acta 35 (11), 1155–1183.

Latham, A.G., 1999. Cave Breccias and Archaeological Sites. Capra 1 available at—http://www.shef.ac.uk/~capra/1/breccia.html.

Latham, A.G., Schwarcz, H.P., 1992. The Petralona Hominid Site—U-series reanalysis of 'Layer 10' calcite and associated palaeomagnetic analyses. Archaeometry 34, 135–140.

Le Cloarec, M.F., Allard, P., Ardouin, B., Giggenbach, W.F., Sheppard, D.S., 1992. Radioactive isotopes and trace elements in gaseous emissions from White Island, New Zealand. Earth and Planetary Science Letters 108 (1–3), 19–28.

Ludwig, K.R., 2003. Mathematical–statistical treatment of data and errors for Th-230/U geochronology. Uranium-Series Geochemistry, Reviews in Mineralogy and Geochemistry, vol. 52, pp. 631–656.

Ludwig, K.R., Titterington, D.M., 1995. Calculation of $^{230}Th/U$ isochrons, ages, and errors. Geochimica et Cosmochimica Acta 58 (22), 5031–5052.

Luo, S., Ku, Teh-Lung, 1991. U-series isochron dating: a generalized method employing total-sample dissolution. Geochimica et Cosmochimica Acta 55 (2), 555–565.

McDermott, F., 2004. Palaeo-climate reconstruction from stable isotope variations in speleothems: a review. Quaternary Science Reviews 23, 901–918.

McDermott, F., Schwarcz, H.P., Rowe, P.J., in press. Isotopes in Speleothems. In: Leng, M., (Ed.) Isotopes in Palaeoenvironmental Research. Springer, Dordrecht, The Netherlands.

Macdougall, J.D., 1995. Using short-lived U and Th series isotopes to investigate volcanic processes. Annual Reviews of Earth and Planetary Science 23, 153–167.

Marshall, J.D., Jones, R.T., Crowley, S.F., Oldfield, F., Nash, S., Bedford, A., 2002. A high resolution late-glacial isotopic record from Hawes Water Northwest England. Climatic oscillations: calibration and comparison of palaeotemperature proxies. Palaeogeography, Palaeoclimatology, Palaeoecology 185, 25–40.

McGarry, S.F., Baker, A., Hawkesworth, C.J., Caseldine, C.J., Smart, P.L., submitted for publication. Speleothem pollen records of warmings during the Last Glaciation in the British Isles. Journal of Quaternary Science.

Millard, A.R., Hedges, R.E.M., 1996. A diffusion–adsorption model of uranium uptake by archaeological bone. Geochimica et Cosmochimica Acta 60 (12), 2139–2152.

Moran, S.B., Shen, C.C., Edmonds, H.N., Weinstein, S.E., Smith, J.N., Edwards, R.L., 2002. Dissolved and particulate Pa-231 and Th-230 in the Atlantic Ocean: constraints on intermediate/deep water age, boundary scavenging, and Pa-231/Th-230 fractionation. Earth and Planetary Science Letters 203 (3–5), 999–1015.

Moran, S.B., Shen, C.-C., Edwards, R.L., Edmonds, H.N., Scholten, J.C., Smith, J.N., Ku, T.-L., 2005. ^{231}Pa and ^{230}Th in surface sediments of the Arctic Ocean: implications for $^{231}Pa/^{230}Th$ fractionation, boundary scavenging, and advective export. Earth and Planetary Science Letters 234, 235–248.

Mortlock, R.A., Fairbanks, R.G., Chui, T.-Z., Rubenstone, J., 2005. $^{230}Th/^{234}U/^{238}U$ and $^{231}Pa/^{235}U$ ages from a single fossil coral fragment by multi-collector magnetic-sector inductively coupled plasma mass spectrometry. Geochimica et Cosmochimica Acta 69 (3), 649–657.

Orloff, K.G., Mistry, K., Charp, P., Metcalf, S., Marino, R., Shelly, T., Melaro, E., Donohoe, A., Jones, R.L., 2005. Human exposure to uranium in groundwater. Environmental Research 95 (5), 319–326.

Palmer, M.R., Edmond, J.M., 1993. Uranium in river water. Geochimica et Cosmochimica Acta 57 (20), 4947–4955.

Petit-Maire, N., Sanlaville, P., Abed, A., Yasin, S., Bourrouilh, R., Carbonel, P., Fontugne, M., Reyss, J.L., 2002. New data for an Eemian lacustrine phase in southern Jordan. Episodes 25 (5), 279–280.

Pike, A.W.G., Hedges, R.E.M., van Calsteren, P., 2002. U-series dating of bone using the diffusion–adsorption model. Geochimica et Cosmochimica Acta 66 (25), 5273–5286.

Pike, A.W.G., Eggins, S., Grün, R., Hedges, R.E.M., Jacobi, R.M., 2005. U-series dating of the late Pleistocene fauna from Wood Quarry (Steetley), Nottinghamshire, UK. Journal of Quaternary Science 20 (1), 59–65.

Platzner, I.T., Habfast, K., Walder, A.J., Goetz, A., 1997. Modern Isotope Ratio Mass Spectrometry, Chemical Analysis, vol. 145. John Wiley and Sons, ISBN: 0-471-97416-1 pp. 1–515.

Pogge von Strandmann, P., Burton, K., James, R., Calsteren, P., Gíslason, S., 2005. The Behaviour of Uranium and Lithium

Isotopes During Basalt Weathering and Erosion. EGU Abstract, EGU05-A-09075.

Potter, E.-K., Stirling, C.H., Wiechert, U.H., Halliday, A.N., Spötl, C., 2005. Uranium-series dating of corals in situ using laser ablation MC–ICPMS. International Journal of Mass Spectrometry 204, 27–35.

Regelous, M., Turner, S.P., Elliott, T.R., Rostami, K., Hawkesworth, C.J., 2004. Measurement of femtogram quantities of protactinium in silicate rock samples by multicollector inductively coupled plasma mass spectrometry. Analytical Chemistry 76 (13), 3584–3589.

Reynolds, B.C., Wasserburg, G.J., Baskaran, M., 2003. The transport of U- and Th-series nuclides in sandy confined aquifers. Geochimica et Cosmochimica Acta 67 (11), 1955–1972.

Robinson, L.F., Henderson, G.M., Slowey, N.C., 2002. U–Th dating of marine isotope stage 7 in Bahamas slope sediments. Earth and Planetary Science Letters 196 (3–5), 175–187.

Shen, G., Cheng, H., Edwards, R.L., 2003. Mass spectrometric U-series dating of New Cave at Zhoukoudian, China. Journal of Archaeological Science 31 (3), 337–342.

Soligo, M., Tuccimei, P., Barberi, R., Delitala, C., Miccadei, E., Taddeucci, A., 2002. U/Th dating of freshwater travertine from Middle Velino Valley (Central Italy): paleoclimatic and geological implications. Palaeogeography, Palaeoclimatology, Palaeoecology 184, 147–161.

Spiegelman, M., Elliott, T., 1993. Consequences of melt transport for Uranium series disequilibrium in young lavas. Earth and Planetary Science Letters 118 (1–5), 1–20.

Staubwasser, M., Henderson, G.M., Berkman, P.A., Hall, B.L., 2004. Ba, Ra, Th, and U in marine mollusc shells and the potential of ^{226}Ra/Ba dating of Holocene marine carbonate shells. Geochimica et Cosmochimica Acta 68 (1), 89–100.

Stirling, C.H., Esat, T.M., McCulloch, M.T., Lambeck, K., 1995. High-precision U-series dating of corals from Western Australia and implications for the timing and duration of the last interglacial. Earth and Planetary Science Letters 135, 115–130.

Thomson, J., Nixon, S., Croudace, I.W., Pedersen, T.F., Brown, L., Cook, G.T., MacKenzie, A.B., 2001. Redox-sensitive element uptake in north-east Atlantic Ocean sediments (Benthic Boundary Layer Experiment sites). Earth and Planetary Science Letters 184 (2), 535–547.

Thomson, J., Green, D.R.H., van Calsteren, P., van Weering T.C.E., submitted for publication. Holocene sediment deposition on Feni Drift (NE Atlantic) and its surrounds quantified by radiocarbon and $230Th_{excess}$ methods.

Thorpe, J., Kristen, I., Leng, M., Mackay, A., Oberhaensli, H., Partridge, T., Thomas, L., Green, J., 2005. Records of Paleoclimatic Change from Tswaing Crater Lake, South Africa. Abstract, PAGES Second Open Science Meeting, 10–12 August 2005. Beijing, China.

Vigier, N., Bourdon, B., Joron, J.L., Allegre, C.J., 1999. U-decay series and trace element systematics in the 1978 eruption of Ardoukoba, Asal rift: timescale of magma crystallization. Earth and Planetary Science Letters 175 (1–2), 81–97.

Villemant, B., Feuillet, N., 2003. Dating open systems by the U-238–U-234–Th-230 method: application to Quaternary reef terraces. Earth and Planetary Science Letters 210 (1–2), 105–118.

Yamamoto, J., Burnhard, P.G., 2005. Solubility controlled noble gas fractionation during magmatic degassing: implications for noble gas compositions of primary melts of OIB and MORB. Geochimica et Cosmochimica Acta 69 (3), 727–734.

Zhao, Jian-xin, Wang, Yong-jin, Collerson, K.D., Gagan, M.K., 2003. Speleothem U-series dating of semi-synchronous climate oscillations during the last deglaciation. Earth and Planetary Science Letters 216, 155–161.